JACS
JOURNAL OF THE AMERICAN CHEMICAL SOCIETY

Article

pubs.acs.org/JACS

Discovery of a Small-Molecule Inhibitor of Protein−MicroRNA Interaction Using Binding Assay with a Site-Specifically Labeled Lin28

Donghyun Lim,[†] Wan Gi Byun,[‡] Ja Young Koo,[‡] Hankum Park,[†] and Seung Bum Park*[,†,‡]

[†]Department of Biophysics and Chemical Biology, Seoul National University, Seoul 08826, Korea

[‡]CRI Center for Chemical Proteomics, Department of Chemistry, Seoul National University, Seoul 08826, Korea

Supporting Information

ABSTRACT: MicroRNAs (miRNAs) regulate gene expression by targeting protein-coding transcripts that are involved in various cellular processes. Thus, miRNA biogenesis has been recognized as a novel therapeutic target. Especially, the let-7 miRNA family is well-known for its tumor suppressor functions and is downregulated in many cancer cells. Lin28 protein binds to let-7 miRNA precursors to inhibit their maturation. Herein, we developed a FRET-based, high-throughput screening system to identify small-molecule inhibitors of the Lin28−let-7 interaction. We employed unnatural amino acid mutagenesis and bioorthogonal chemistry for the site-specific fluorescent labeling of Lin28, which ensures the robustness and reliability of the FRET-based protein−miRNA binding assay. Using this direct binding assay, we identified an inhibitor of the oncogenic Lin28−let-7 interaction. The inhibitor enhanced the production of let-7 miRNAs in Lin28-expressing cancer cells and reduced the level of let-7 target oncogene products.

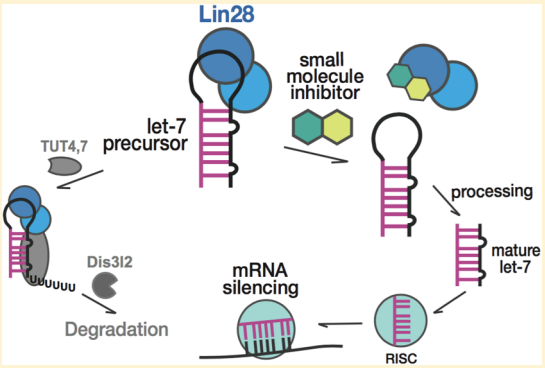

INTRODUCTION

MicroRNAs (miRNAs) are small noncoding RNAs that regulate gene expression by acting as guide molecules in RNA silencing.[1] They function through base pairing with their target messenger RNAs (mRNAs) usually at the 3′ untranslated region (UTR). This interaction leads to translational repression, mRNA deadenylation, and mRNA decay.[1,2] In the nucleus, miRNAs are initially transcribed as long primary miRNAs (pri-miRNAs). These transcripts are cleaved by the RNase III enzyme Drosha to form precursor miRNAs (pre-miRNAs) with 60−80 nucleotide-long stem-loop structures. Pre-miRNAs are then transported to the cytoplasm, where they are processed by Dicer to form mature miRNAs.[3,4] Biogenesis of miRNAs is tightly regulated both temporally and spatially, and its dysregulation is closely associated with many human diseases.[1,3,5,6] Therefore, miRNA biogenesis has been emerging as a novel therapeutic target. In fact, miRNAs are able to concurrently modulate multiple genes in a single cellular pathway or multiple genes in multiple pathways, which makes them efficient drug targets as exemplified by miR-181 that controls multiple phosphatases in T lymphocytes.[5,7] Moreover, targeting miRNA biogenesis can be one of the best options when the proteomes of certain cellular pathways are intractable by conventional methods.[8]

Let-7 miRNAs play important roles in cellular differentiation during development and act as tumor suppressors by targeting multiple oncogenic proteins such as c-Myc, HMGA2, and Ras.[9−11] They are ubiquitously expressed in normal cells but are down-regulated in many cancer cells, leading to poor prognosis in patients.[12,13] Tumor growth was shown to be suppressed by the delivery of let-7 into cancer cells both in vitro and in vivo.[10,14,15] The RNA-binding protein Lin28 was shown to selectively block let-7 biogenesis at the post-transcriptional level.[16] Mammals have two Lin28 paralogs: Lin28A and Lin28B. They bind primary let-7 (pri-let-7) and precursor let-7 (pre-let-7) at the terminal loop, which then blocks miRNA processing by Drosha and Dicer, respectively.[15,17] Lin28 also mediates the degradation of pre-let-7 by recruiting terminal uridyltransferases (TUTs) to produce oligouridylated pre-let-7 which is cleared by a nuclease Dis3l2 (Figure 1a).[18]

The cellular level of Lin28 is inversely correlated with the level of mature let-7 miRNA. Lin28 is highly expressed in stem cells, but is not detected in normal differentiated somatic cells. However, Lin28 is abnormally expressed in many cancer cells, concomitant with the reduced let-7 expression.[17,19] Knock-down of Lin28 in cancer cells restored let-7 levels and inhibited tumor growth.[15] In particular, a growing body of evidence suggests that Lin28 plays a crucial role in the maintenance of cancer stem cells, contributing to drug resistance, tumor recurrence, and metastasis.[17,20−24] Thus, antagonizing the action of Lin28 and restoring let-7 expression could be a

Received: July 6, 2016
Published: September 26, 2016

DOI: 10.1021/jacs.6b06965
J. Am. Chem. Soc. 2016, 138, 13630−13638

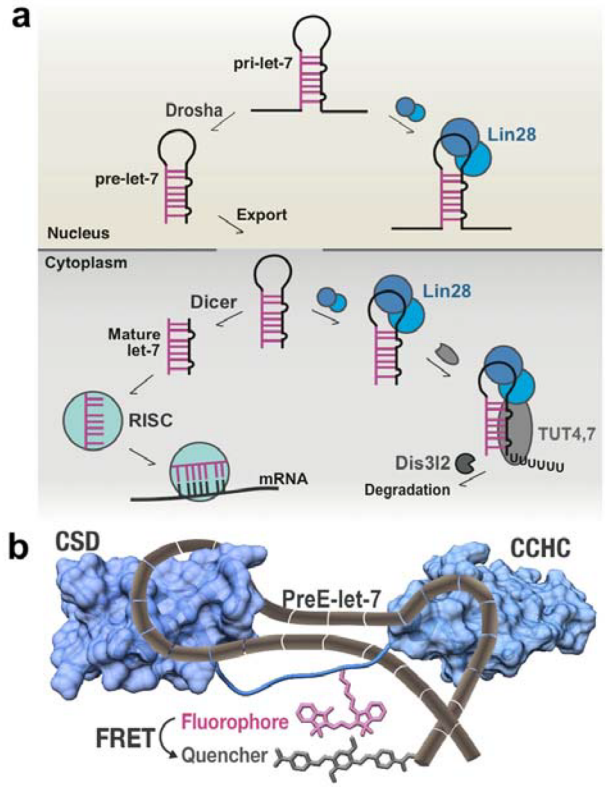

Figure 1. (a) Regulation of let-7 miRNA biogenesis. RISC, RNA-induced silencing complex. (b) Schematic model of Lin28–let-7 binding and our design strategy for constructing a FRET-based binding assay.

novel strategy to treat cancer. Delivery of let-7 mimics or siRNA against Lin28 is a basic approach to restore the let-7 levels.[10,14,15] Antagonizing the interaction between Lin28 and let-7 precursors using short oligoribonucleotides[25] or small molecules[26,27] can be another option. However, oligonucleotides are limited in use due to their poor cellular delivery and nonspecific stimulation of the immune system.[28] Therefore, we aimed to develop a novel high-throughput Lin28–let-7 binding assay to identify small-molecule inhibitors of this protein–miRNA interaction.

For our small-molecule screening, we aimed to develop a homogeneous, direct binding assay in a high-throughput format that would minimize any RNA degradation arising from multiple addition/washing steps. Herein, we describe a new protein–miRNA binding assay based on Förster resonance energy transfer (FRET). In FRET, a donor molecule in its excited state can transfer energy to an acceptor molecule through a nonradiative mechanism when they are in close proximity (<100 Å). Because FRET efficiency is proportional to the inverse of the sixth power of the distance between the donor and the acceptor, the FRET signal is sensitive to small changes in distance.[29,30] Thus, FRET is a powerful tool for studying the direct interactions between biopolymers.

To build a direct binding assay, the interaction partners are labeled with light-sensitive FRET donor–acceptor pairs. However, current labeling strategies are limited to fusion with fluorescent proteins or random chemical modification with organic fluorophores. The relatively large size of fluorescent proteins may hamper direct interactions between biomolecules. In addition, fluorescent proteins are fused at either the *N*- or *C*-terminus of the protein of interest, which makes it difficult to control the distance between FRET partners and consequently FRET efficiency.[31] Actually, a recently developed FRET assay using EGFP-tagged Lin28B only showed a moderate FRET efficiency, even after testing various let-7a-2 precursors labeled with FRET acceptors.[26,27] Random chemical modification by organic fluorophores through the amine, acid, or thiol functionalities of the proteins can also disrupt the biomolecular interaction due to the labeling at binding site residues.[32] Moreover, the heterogeneity in the dye-to-protein ratio and the distances from dye-labeled residues of the proteins to FRET acceptors may not provide consistent FRET signals.

Therefore, we employed site-specific unnatural amino acid mutagenesis and bioorthogonal chemistry to generate a precisely designed fluorescent Lin28. The combination of the Lin28 protein site-specifically labeled with an organic fluorophore and quencher-labeled let-7 miRNA should guarantee high FRET efficiency by ensuring close proximity between the fluorophore and the quencher, ultimately leading to a robust and reliable binding assay. This assay platform was used to identify a small-molecule inhibitor of the Lin28–let-7 interaction. We also investigated the cellular activity and the mode of action of this protein–miRNA interaction inhibitor.

RESULTS AND DISCUSSION

Design Strategy for a New FRET Assay to Detect Lin28–let-7 Interaction. Simple, fast, and reliable homogeneous binding assays for identifying novel modulators of biomolecular interactions in a high-throughput manner are in high demand. A FRET-based assay is an ideal option for the Lin28–let-7 interaction, especially in comparison with fluorescence polarization (FP) assays, which are limited by the molecular weight differences required to detect the signal. In addition, FRET assays can be easily conducted using standard laboratory equipment.[30]

We set out to develop a new FRET-based assay with high FRET efficiency in order to achieve a wide signal window. To this end, the FRET donor and the acceptor should be in close proximity, and an efficient donor–acceptor pair with maximal overlap between the emission spectra of the donor and the absorption spectra of the acceptor should be selected. To fulfill these criteria, we designed and generated Cy3-labeled Lin28 and BHQ-2-labeled let-7 miRNA. The labeling sites in the protein and RNA were selected based on the cocrystal structure of Lin28A with three different let-7 terminal loops.[33] As shown in Figure 1b, Lin28 has two domains, the cold shock domain and the tandem CCHC-type zinc finger connected by a flexible linker. Both domains are responsible for specific binding to let-7 miRNAs at their terminal loop region, termed the pre-element (preE). The mature miRNA region is not required, but the preE is sufficient for specific binding. There are 12 reported subtypes in the let-7 miRNA family, 11 of which bind Lin28 specifically due to their consensus binding sequences. Finally, the Lin28 linker has a net positive charge that might aid in the binding of negatively charged RNAs. However, the linker is not essential for specific binding, and a portion of the linker can be deleted without compromising binding events.[17,33–35]

Close examination of the crystal structures showed that the Lin28A linker and the 3′ end of preE-let-7 are close to each other. Therefore, we tried to site-specifically label Lin28A with Cy3 in the linker region and synthesize preE-let-7a-1 labeled with BHQ-2 at its 3′ end. When the labeled RNA binds to Lin28A, the Cy3 fluorescence is quenched because of its

DOI: 10.1021/jacs.6b06965
J. Am. Chem. Soc. 2016, 138, 13630–13638

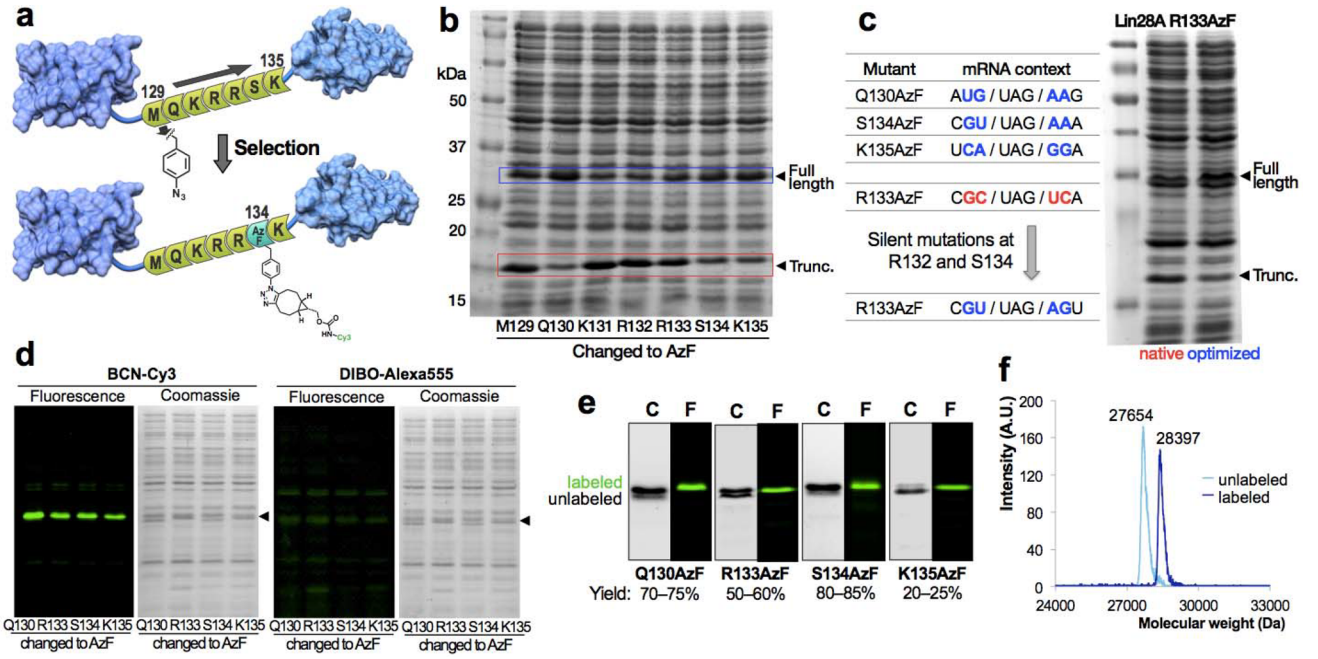

Figure 2. (a) Schematic diagram of the optimized production of Lin28A-Cy3 from the scanning mutagenesis of the Lin28A linker residues. (b) SDS-PAGE data from the scanning mutagenesis. Full-length proteins and truncated proteins are marked with blue and red boxes, respectively. (c) The optimization of mRNA context to enhance the production of full-length R133AzF mutant. (d) Labeling of crude lysates from four Lin28A AzF mutant cultures with either BCN-Cy3 or DIBO-Alexa555. Arrowheads indicate Lin28A AzF mutants. (e) Labeling of purified Lin28A AzF mutants with BCN-Cy3. C, Coomassie; F, Fluorescence. (f) MALDI-TOF analysis of Lin28A S134AzF before and after the labeling reaction. Expected mass difference, 749 Da; observed mass difference, 743 Da.

proximity to BHQ-2; however, in the presence of small-molecule interaction inhibitors, the Cy3 fluorescence can be detected. This binding inhibition assay is therefore a turn-on assay. Because the site-specific RNA synthesis is straightforward, we focused on the production of Lin28A labeled with Cy3 in the linker region. Lin28A contains many lysine and cysteine residues, some of which have key roles in RNA binding or are part of important structural motifs.[33] Therefore, conventional chemical labeling using *N*-hydroxysuccinimide or maleimide is not appropriate, which led us to introduce an unnatural amino acid into the linker region of Lin28A and label it with a Cy3 fluorophore through bioorthogonal chemistry. Specifically, we chose copper-free [3 + 2] cycloaddition of azide with cyclooctyne owing to its selectivity and high reaction rate under mild physiological conditions. Thus, we set out to introduce the unnatural amino acid 4-azido-L-phenylalanine (AzF) into Lin28A.

Site-Specific Fluorescent Labeling of Lin28A through Unnatural Amino Acid Mutagenesis. AzF can be site-specifically incorporated into a protein of interest by reassigning the amber stop codon (UAG) to encode an unnatural amino acid.[36] A plasmid (pEVOL-AzF) encoding orthogonal $tRNA_{CUA}$ and the aminoacyl tRNA synthetase (aaRS) for AzF[37] was cotransformed into *E. coli* along with a plasmid encoding Lin28A that contains an amber mutation at the desired residue in order to express a AzF mutant. Initially, we designed three different *N*-terminal 6 × His-tagged Lin28A linker mutants (K131AzF, R133AzF, and K135AzF), and we expressed and purified them by nickel affinity chromatography. However, only small amounts of full-length AzF mutants were obtained, while the majority of the protein produced was a truncated form of Lin28A due to the amber codon acting as a stop signal (Figure S1). Competition between amber suppression and translational termination is a major hurdle in unnatural amino acid mutagenesis. A simple approach to solve this problem is to attach the purification tag at the *C*-terminus of the protein. However, in the case of Lin28A, despite several attempts, it was not possible to obtain functional *C*-terminal His-tagged protein.

Several other methods were used to attempt to increase the amber suppression efficiency, including release factor 1 knockout or elongation factor-Tu engineering in *E. coli*.[38,39] However, these methods require complicated genetic engineering to obtain specialized strains. More importantly, there is no general rule for increasing amber suppression over translational termination in normal expression strains such as *E. coli* BL21(DE3). Therefore, we set out to optimize the culture conditions for maximal amber read-through in BL21(DE3), using Lin28A K135AzF as a model mutant, which would then enable the production of a Lin28 AzF mutant through a single affinity chromatography step. We found that the culture temperature significantly affected the amber suppression efficiency. Higher temperatures increased the ratio of full-length protein to truncated protein, mainly through a substantial decrease in translational termination rather than an increase in read-through (Figure S2a). Thus, the culture temperature was set to be 37 °C. Following this, the effects of other culture conditions were investigated. Changes in the concentrations of arabinose, for aaRS induction, and of IPTG, for Lin28A induction, had minor effects over the ranges tested (Figure S2b). It was found to be beneficial to induce aaRS before inducing Lin28A in order to ensure that the AzF-charged $tRNA_{CUA}$ was present when Lin28A was first expressed (Figure S2c). Finally, by optimizing the culture conditions, we were able to efficiently produce Lin28A K135AzF.

DOI: 10.1021/jacs.6b06965
J. Am. Chem. Soc. 2016, 138, 13630−13638

We then used scanning mutagenesis to obtain seven Lin28A linker mutants under the optimized conditions (Figure 2a) and tried to identify the best Cy3 labeling site for the assay. However, only three of the mutants (Q130AzF, S134AzF, and K135AzF) were efficiently produced (Figure 2b). We then sought to increase the yield of full-length protein by changing the mRNA context of the amber codon. In *E. coli*, there is a bias in mRNA sequences several nucleotides before and after stop codons, indicating that termination efficiency is closely related to the mRNA context of the stop codons.[40] Accordingly, we expected that the amber suppression efficiency would also be dependent on the mRNA context when the exogenous orthogonal $tRNA_{CUA}$ was employed to insert an unnatural amino acid. However, there is no published information about the preferred mRNA sequences before and after the amber codon. We were able to extract some information about nucleotide preference from our own scanning mutagenesis experiment with Lin28A (Figure 2c). Using this information, we made silent mutations in two nucleotides before and after the amber codon in Lin28A R133AzF, which improved the production of the full-length protein by >2 fold (Figure 2c).

We proceeded to conjugate the fluorescent label to the mutant proteins using copper-free strain-promoted cycloaddition, which is a mild and efficient transformation method.[41] First, crude cell lysates from *E. coli* containing four Lin28A mutants were labeled with either bicyclononyne-Cy3 (BCN-Cy3) or dibenzocyclooctyne-Alexa555 (DIBO-Alexa555). As shown in Figure 2d, the labeling efficiency of BCN-Cy3 was much higher than that of DIBO-Alexa555. In addition, BCN-Cy3 labeled Lin28A in a highly selective manner, whereas the labeling with DIBO-Alexa555 yielded multiple nonspecific fluorescent signals. Therefore, we selected BCN-Cy3 for the site-specific fluorescence labeling of Lin28A AzF mutants. Next, we labeled the four different purified Lin28A mutants with BCN-Cy3. The labeling efficiency ranged from 20% to 85% depending on the labeling site (Figure 2e), which was calculated based on the intensities of the Coomassie-stained protein bands after SDS-PAGE. S134AzF was most efficiently labeled with Cy3. The bioorthogonal copper-free click reaction led to single-site labeling of Lin28A through the azide moiety of AzF, which was confirmed by MALDI-TOF analysis of the unlabeled and labeled Lin28A S134AzF protein (Figure 2f). In contrast, random chemical labeling with *N*-hydroxysuccinimide-Cy3 (NHS-Cy3) at the primary amine moiety resulted in a heterogeneous protein population, as evidenced by smearing of the Cy3-labeled protein band in SDS-PAGE and the wider distribution of the MALDI-TOF spectrum (Figure S3a and b). Therefore, the Lin28A S134AzF mutant labeled with BCN-Cy3 (Lin28A-Cy3) was used to develop a FRET-based assay to monitor the protein−miRNA interaction.

FRET-Based Direct Binding Assay between Lin28A and let-7. To maximize the signal window for quantifying the protein−RNA interaction, we designed a robust and reliable screening strategy using the FRET quenching mechanism by placing the FRET donor and quencher in close proximity. We constructed a FRET-based screening platform using Lin28A-Cy3 and preE-let-7a-1-BHQ-2 as a model to identify small-molecule inhibitors of the protein−miRNA interaction. Our turn-on assay platform was evaluated by adding a solution of preE-let-7a-1-BHQ-2 to a solution of Lin28A-Cy3 predispensed in a screening plate, and measuring the Cy3 fluorescence. As shown in Figure 3a, we observed a sharp decrease in the Cy3 signal when Lin28A-Cy3 was incubated with preE-let-7a-1-BHQ-2; however, in the presence of excess unlabeled preE-let-7a-1, the Cy3 signal was substantially restored. The degree of fluorescence quenching was dependent on the concentration of preE-let-7a-1-BHQ-2, and the FRET quenching efficiency was as high as 85% (Figure 3b). Competition by unlabeled preE-let-7a-1 clearly restored the fluorescence signal from Lin28A-Cy3 in a dose-dependent manner, while a yeast tRNA could not effectively compete with preE-let-7a-1-BHQ-2 bound to Lin28A-Cy3, even at high concentrations (Figure 3c). These results indicated that our assay specifically detects the Lin28A−preE-let-7a-1 interaction. In contrast, a FRET-based assay using Lin28A labeled with NHS-Cy3 exhibited a moderate FRET efficiency (47% using $Lin28A_{native}$NHS-Cy3 vs 79% using $Lin28A_{S134AzF}$BCN-Cy3) and lower specificity toward let-7 miRNA, demonstrating the superiority of our site-specific protein labeling strategy for enhancing the signal window and preserving the biological function of target proteins (Figure S3c and d).

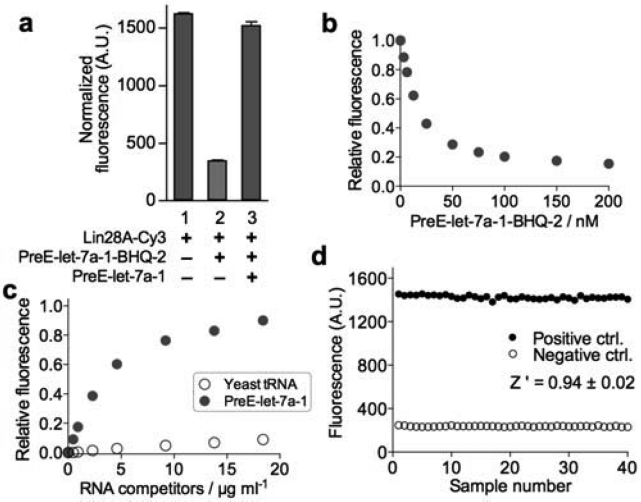

Figure 3. Validation of the binding assay. (a) Competition by excess unlabeled preE-let-7a-1 restores the fluorescent signal. Twenty-five nM Lin28A-Cy3, 50 nM preE-let-7a-1-BHQ-2, and 2 μM competitor were used. (b) Dependence of the relative fluorescence intensity on the preE-let-7a-1-BHQ-2 concentration. Twenty-five nM Lin28A-Cy3 was used. (c) Competition by unlabeled preE-let-7a-1 or yeast tRNA to check the specificity of the assay. Twenty-five nM Lin28A-Cy3 and 50 nM preE-let-7a-1-BHQ-2 were used. (d) Determination of the Z′ factor.

A simple mix-and-read format makes it possible to conduct the binding assay in a high-throughput manner. We performed this FRET-based binding assay using a 96-well half area nonbinding black plate in a high-throughput setting. The Z′ factor was determined using 40 positive controls (samples without preE-let-7a-1-BHQ-2) and 40 negative controls (samples with preE-let-7a-1-BHQ-2) to assess the quality of the screening system.[42] The average Z′ factor of our direct binding assay with Lin28A-Cy3 was 0.94 (Figure 3d). In contrast, the binding assay using Lin28A labeled with NHS-Cy3 showed lower Z′ factor (0.73, Figure S3e). Considering the fact that assays with Z′ factors larger than 0.75 are regarded as excellent, our assay is highly robust, reliable and close to an ideal screening system.

Identification of a Small-Molecule Inhibitor of the Lin28−let-7 Interaction and Its Cellular Activity. Our FRET-based high-throughput screening system was applied to identify small-molecule inhibitors of the Lin28−let-7 inter-

DOI: 10.1021/jacs.6b06965
J. Am. Chem. Soc. 2016, 138, 13630−13638

action from an in-house, 4500-member library of drug-like compounds, constructed by privileged substructure-based diversity-oriented synthesis strategy.[43] Several compounds restored the Cy3 signal when added to the protein−miRNA mixture, and they were validated through an independent secondary method, the electrophoretic mobility shift assay (EMSA). EMSA is based on the difference in the electrophoretic mobility of an RNA and a protein−RNA complex. The mobility of an RNA is greatly retarded when it is bound to a protein due to the increased mass-to-charge ratio, which allows direct measurement of the amount of free RNA and protein-bound RNA.[44] The identified inhibitors of the Lin28−let-7 interaction should therefore increase the ratio of the RNA band to the protein−RNA band. We performed the EMSA using a recombinant native Lin28A and preE-let-7a-1 labeled with Cy5 at its 5′-terminus (Cy5-preE-let-7a-1). Lin28A and preE-let-7a-1 formed a complex that was differentiated by native PAGE. The Lin28−Cy5-preE-let-7a-1 interaction was clearly abolished in the presence of the unlabeled competitor preE-let-7a-1 in a dose-dependent manner (Figure S4).

From the high-throughput screening and EMSA-based confirmation, we identified a benzopyranylpyrazole-based hit compound **1**, which showed a clear antagonistic effect against the Lin28A−let-7a-1 interaction with IC_{50}s in the micromolar range in these assays (Figure 4a−c). It was possible to observe a

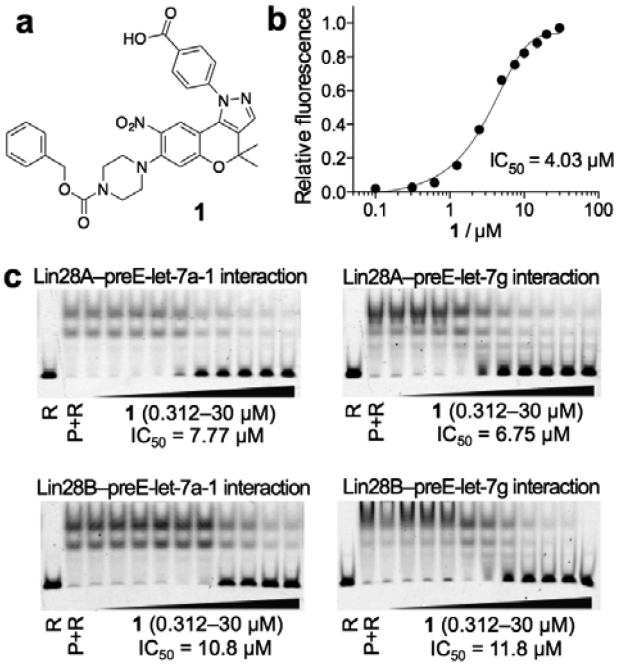

Figure 4. Identification of a hit compound and verification by EMSA. (a) Structure of hit compound **1** identified from our FRET-based high-throughput assay. (b) **1** restored fluorescence signal in the FRET assay. (c) **1** inhibited Lin28A−preE-let-7a-1, Lin28A−preE-let-7g, Lin28B−preE-let-7a-1, and Lin28B−preE-let-7g interactions. R, RNA; P, Protein.

limited range of structure−activity relationship for the initial hit compound, because our in-house screening library contains several compounds with the benzopyranylpyrazole core.[45] A carboxylic acid functionality attached to the pyrazole-connected phenyl ring is essential for the inhibitory effect. Compounds with different substituents (**2**−**6**) did not exhibit any activity against the protein−RNA interaction (Figure S5a and b). In order to further investigate the substituent effects at the pyrazole ring, we evaluated a small set of synthetic analogues (**7**−**10**). In EMSA (Figure S5a and c), we did not observe any inhibitory effect against the protein−miRNA interaction among these analogues (**2**−**10**). Especially, shifting the carboxylic acid moiety from *para*- (**1**) to *meta*-position (**9**) completely abolished the inhibitory activity. Masking the acid functionality of **1** through the formation of methyl ester (**10**) also eliminated the inhibitory effect, emphasizing the importance of carboxylic acid moiety located at the *para*-position relative to the pyrazole ring.

Given the high sequence homology and structural similarity between Lin28A and Lin28B,[15] the inhibitory effect of the hit compound **1** against the Lin28B−let-7 interaction was also assessed by EMSA using recombinant Lin28B and Cy5-PreE-let-7a-1 as a probe. As expected, **1** also inhibited the Lin28B−let-7 interaction, with slightly reduced potency (Figure 4c). In fact, many cancer cells exclusively express either Lin28A or Lin28B.[15,17] Therefore, selective small-molecule inhibitors against both Lin28A−let-7 and Lin28B−let-7 interactions are highly desirable for treating a wide range of cancers. There are 11 human let-7 family members whose processing is blocked by binding to Lin28. The binding between Lin28 and each of the let-7 family members is expected to proceed in an almost identical manner.[17,33,34] Ideally, inhibitors should disrupt all the Lin28−let-7 interactions in order to rapidly and substantially increase the cellular levels of mature let-7. We found that **1** also inhibits the Lin28A−let-7g and Lin28B−let-7g interactions with similar IC_{50} values (Figure 4c). Therefore, **1** might be a good starting point for designing novel inhibitors of the protein−RNA interaction.

To elucidate the inhibitory mechanism of the active compound, we performed biophysical studies using surface plasmon resonance (SPR), which showed that **1** clearly binds to Lin28A, whereas compounds without inhibitory effects (**2**−**4**) exhibited very weak binding to Lin28A (Figures 5a and S6). In addition, differential scanning fluorimetry was performed to detect the thermal stabilization of Lin28A upon engagement of

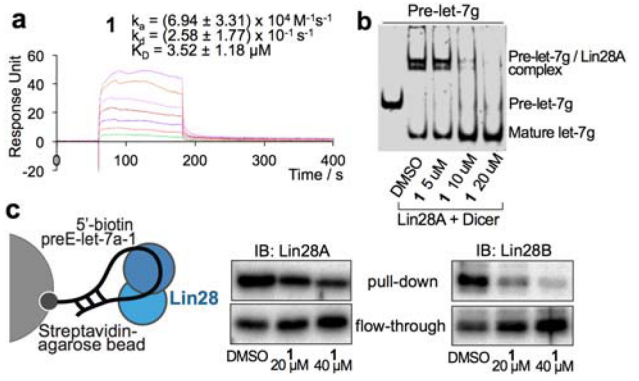

Figure 5. (a) SPR analysis of the direct binding between Lin28A and **1** using a Biacore T100 instrument. **1** was used at concentrations from 1.25 μM to 20 μM. (b) In vitro Dicer processing assay. 5′-phosphate-pre-let-7g was incubated with Dicer and Lin28A in the absence or presence of **1**. The reaction mixtures were resolved by native gel electrophoresis, and the RNAs were visualized by SYBR green II staining. (c) RNA pull-down experiment using biotinylated preE-let-7a-1 and lysates from JAR cells. RNA-bound fraction (pull-down) and unbound fraction (flow-through) were resolved by SDS-PAGE and probed for Lin28A and Lin28B through immunoblotting.

DOI: 10.1021/jacs.6b06965
J. Am. Chem. Soc. 2016, 138, 13630−13638

the hit compound. The results indicated that the Lin28A melting temperature (T_m) was increased by more than 2.0 °C in the presence of **1**. On the other hand, inactive compounds **2** and **4** increased the T_m by less than 0.4 °C, which corresponds well to the results obtained from the SPR analysis (Table S1). Collectively, **1** inhibits Lin28A−let-7 interaction by binding to the protein partner. Next, we attempted to identify a protein domain responsible for the binding to **1**. Therefore, the cold shock domain (CSD, residues 1−119) and the CCHC-type zinc finger domain (ZFD, residues 126−184) were separately expressed and their independent binding toward **1** was recorded using SPR analysis. As shown in Figure S7, the interaction of **1** toward CSD generated clear concentration-dependent SPR signals. On the other hand, binding analysis between ZFD and **1** did not generate meaningful signals. Therefore, **1** inhibits Lin28−let-7 interaction by mainly binding to the CSD of Lin28. Because both CSD and ZFD are required for high-affinity binding toward let-7 family,[33] specific binding of **1** to CSD is enough to dissociate let-7 miRNAs from Lin28 protein.

On the basis of the miRNA biogenesis pathway, pre-let-7 dissociated from Lin28 would be processed by Dicer, resulting in the formation of mature miRNA. As shown in Figure 5b, the in vitro Dicer processing assay revealed that compound **1** clearly blocked the formation of the Lin28A−pre-let-7g complex and induced miRNA processing, resulting in the generation of mature let-7g miRNA. Next, we investigated the potential of **1** for disrupting the protein−miRNA interaction in the more complex cellular context through an RNA pull-down assay. Biotinylated preE-let-7a-1 was immobilized on streptavidin-agarose beads, and the beads were incubated with the lysate from JAR cells—a human choriocarcinoma cell line that expresses both Lin28A and Lin28B. The pull-down assay revealed that endogenous Lin28A and Lin28B efficiently bind the RNA. However, the interaction between the protein and the RNA was abolished in the presence of **1**, as demonstrated by the decrease in RNA-bound Lin28A/Lin28B (pull-down) and the increase in RNA-unbound Lin28A/Lin28B (flow-through) (Figure 5c).

Having found that **1** can disrupt the protein−miRNA interaction in a cellular environment, we next investigated the effect of **1** on the cellular levels of mature let-7 in the JAR cell line using quantitative RT-PCR (qRT-PCR) based on the TaqMan miRNA assay. As shown in Figure 6, **1** increased the levels of all mature let-7 family members investigated in this study (let-7a, let-7d, let-7f, let-7g, let-7i, and miR-98). On the other hand, the cellular levels of miRNAs unrelated with Lin28 expression were not affected by **1** (miR-20b and miR-214).

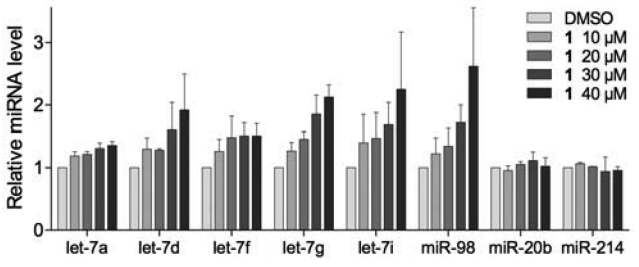

Figure 6. Quantification of mature let-7 levels following 24 h-treatment of JAR cells with **1**. U6 snRNA was employed as an endogenous control. Error bars represent s.d. from at least three independent experiments.

Recently, it was reported that a single let-7 family member, human let-7a-3, can bypass Lin28-mediated regulation because the precursor of let-7a-3 binds Lin28 with much lower affinity compared to the other let-7 precursors. As a result, the cellular level of mature let-7a, which is generated from three precursors (pre-let-7a-1, pre-let-7a-2, and pre-let-7a-3), is less sensitive to Lin28 expression.[35] In accordance with these findings, the cellular level of let-7a was less sensitive to treatment with **1** compared to the other let-7 family members (Figure 6). In addition, Lin28 can bind the precursors of other subsets of miRNAs and regulate their biogenesis, which is similar to the regulation of let-7 biogenesis. Among those miRNAs, we selected five experimentally valdiated targets[9,46,47] and measured the cellular levels of their mature forms upon treatment of JAR cells with **1**. However, two of them (miR-143 and miR-363) were not reliably detected due to their low copy numbers. Therefore, the cellular levels of three miRNAs (miR-9, miR-107, and miR-200c) were investigated. As shown in Figure S8, cellular levels of the three miRNAs were slightly enhanced by **1**. However, the observed increase is substantially smaller than that of let-7 miRNA family. In the previous reports,[9,46] cellular levels of the three miRNAs were increased upon siRNA-mediated Lin28A knock-down, but the net increase of those miRNAs was not as significant as that of let-7 miRNAs, which is consistent with our observation. Therefore, we can assume that **1** can block the association between Lin28 and other miRNAs when their binding modes are similar to that of let-7 miRNA family.

We then examined how the cellular activity of **1** was affected by different expression levels of Lin28. When the expression of both Lin28A and Lin28B were knocked-down using siRNA in JAR cells, the **1**-induced increase in cellular let-7 levels was clearly attenuated. (Figure 7a and b). Compound **1** increased mature let-7 levels in PA-1 cells that express high level of Lin28A. On the other hand, let-7 levels were not affected by **1** in MCF7 cells that rarely express Lin28 proteins (Figure 7c and d). As shown in Figure S5d, we also observed no noteworthy

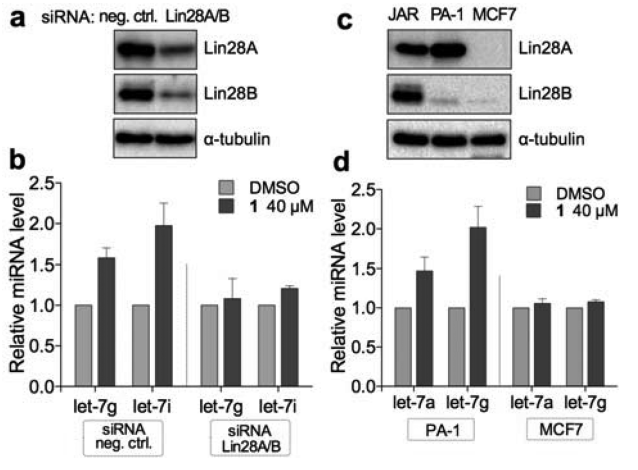

Figure 7. (a) Knock-down of Lin28A and Lin28B expression following siRNA treatment for 72 h. (b) The effect of **1** on mature let-7 levels in the siRNA-treated JAR cells. Cells were incubated with **1** for 24 h. Error bars represent s.d. from three independent experiments. (c) Expression of Lin28 in JAR, PA-1, and MCF7 cell line. (d) The effect of **1** on the mature let-7 levels in PA-1 and MCF7 cells. Cells were incubated with **1** for 24 h. Error bars represent s.d. from three independent experiments.

DOI: 10.1021/jacs.6b06965
J. Am. Chem. Soc. 2016, 138, 13630−13638

changes of the cellular let-7 levels in JAR cells upon treatment with its synthetic analogues (**2**−**10**). Taken together, **1** specifically induces the increase in the cellular let-7 levels by targeting Lin28.

Next, a dual luciferase reporter gene assay was performed to examine whether the let-7 target gene was repressed upon treatment with **1**. JAR cells were transfected with the reporter luciferase vector (WT) containing two let-7 complementary target sites derived from 3′ UTR of n-Myc gene.[48] Cells were also transfected with the control reporter plasmid (m1/2) in which all let-7 target sites were mutated in order to disrupt the pairing with let-7. As shown in Figure 8a, the presence of

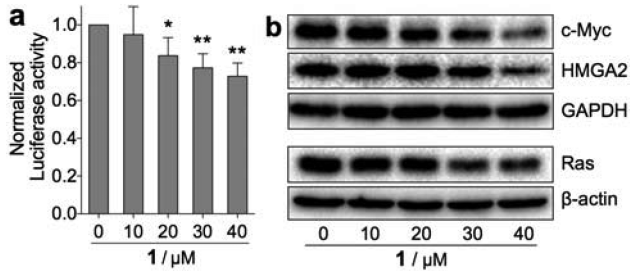

Figure 8. (a) Luciferase reporter gene assay to show the repression of target genes following 24 h-treatment of JAR cells with **1**. The activity of the WT reporter was normalized to that of the m1/2 reporter. Error bars represent s.d. from five independent experiments (*P < 0.05, **P < 0.01, paired two-tailed t-test). (b) Western blot analysis to examine the effect of **1** on the expression of endogenous oncogenic let-7 target gene products in JAR cells. Cells were incubated with **1** for 30 h.

compound **1** decreased the relative expression of let-7 target luciferase in a concentration-dependent manner. Finally, the endogenous levels of let-7 target gene products were measured by Western blot following treatment with **1** in JAR cells. As expected, compound **1** caused a reduction in the levels of the well-validated let-7 target oncogenic proteins, c-Myc, HMGA2, and Ras (Figures 8b and S9).

CONCLUSION

As our understanding of RNA tertiary structure improves and the number of RNA-binding chemical entities increases, RNA is emerging as a viable target for small-molecule drugs, beyond the conventional antibiotic-targeted bacterial rRNAs.[8,28,49] At the same time, protein−RNA interactions, which were once regarded as undruggable, are increasingly becoming recognized as an important class of drug targets. However, to date there have been only a small number of reports regarding small-molecule modulators of protein−RNA interactions, the majority of which target the HIV-1 viral RNAs or expanded nucleotide repeats.[8,49,50] Proteins binding to miRNAs are key components in the determination of miRNA function, because they control many stages of miRNA biogenesis, localization, degradation, and activity.[3] However, there exist only a few reports regarding small molecules that target protein−miRNA interaction. In this study, we constructed a FRET-based high-throughput assay to identify small-molecule inhibitors of the Lin28−let-7 interaction, a protein−miRNA interaction with a promising therapeutic potential. Our FRET-based turn-on assay, developed through a novel design strategy employing site-specific protein labeling by unnatural amino acid mutagenesis, was highly robust and reliable. To the best of our knowledge, this is the first description of a high-throughput biomolecular interaction assay employing an unnatural amino acid-incorporated protein. We identified a benzopyranylpyrazole-based compound as a small-molecule inhibitor of the oncogenic Lin28−let-7 interaction. Biophysical analysis confirmed that the inhibitory effect was mediated by binding between the hit compound and Lin28. We then demonstrated the cellular activity of the protein−miRNA interaction inhibitor through quantification of the miRNA using qRT-PCR, a reporter gene assay, and Western blot analysis. Our hit compound **1** could be used as a lead to design novel inhibitors of the Lin28−let-7 interaction with enhanced activity. In addition, our site-specific protein labeling strategy could be applied to construct different types of high-throughput binding assays.

EXPERIMENTAL SECTION

Protein Expression and Purification. *N*-terminal 6 × His-tagged native human Lin28A and Lin28B were overexpressed in *E. coli* Rosetta2 (DE3) pLysS. The cells were grown to optical density at 600 nm of 0.6−0.8. Protein expression was induced with 0.5 mM IPTG overnight at 18 °C. Cell pellets were resuspended in cold lysis buffer (20 mM Tris·HCl, pH 8.0, 500 mM NaCl, 10 mM imidazole, 1× protease inhibitor cocktail, 1 mM PMSF, 1 mM DTT, 50 μM $ZnCl_2$, 10% glycerol) and sonicated. The lysate was cleared through centrifugation followed by filtering. The filtrate was incubated with Ni-NTA agarose beads [Qiagen] for 1.5 h at 4 °C. The beads were washed with 80 bead volumes of wash buffer A (20 mM Tris·HCl, pH 8.0, 500 mM NaCl, 20 mM imidazole, 50 μM $ZnCl_2$, 10% glycerol), then 30 bead volumes of wash buffer B (20 mM Tris·HCl. pH 8.0, 500 mM NaCl, 50 mM imidazole, 50 μM $ZnCl_2$, 10% glycerol). The proteins were eluted with 8 bead volumes of elution buffer (20 mM HEPES, pH 7.5, 500 mM NaCl, 100−300 mM imidazole, 10% glycerol). Imidazole was removed using a PD-10 column [GE Healthcare] to provide the protein solution in dialysis buffer (20 mM HEPES, pH 7.5, 500 mM NaCl, 10% glycerol). The protein was aliquoted in small fractions, snap-frozen in liquid nitrogen, and stored at −80 °C. Protein expression was verified through mass spectrometry and Western blot analysis.

Unnatural Amino Acid Mutagenesis. Mutant human Lin28A with an unnatural amino acid was expressed in *E. coli* BL21(DE3) after codon optimization at 4 residues (R122, R133, R138, and L145) for efficient protein expression. Site-directed mutagenesis was performed to introduce an amber codon at the linker region of Lin28A. *E. coli* BL21(DE3) was cotransformed with the amber mutant plasmid and pEVOL-AzF that encodes an orthogonal tRNA−aaRS pair.[37] The cells were grown to an optical density at 600 nm of 0.6, and 1.5 mM AzF and 0.06% arabinose were added to produce AzF-charged orthogonal tRNA. After incubation for an hour at 37 °C, Lin28A expression was induced with 0.25 mM IPTG for 6 h at 37 °C. The protein purification procedure was the same as that used for native Lin28.

Fluorescent Labeling. Cleared lysate from 50 mL of *E. coli* culture containing Lin28A AzF mutants was incubated with 120 μL Ni-NTA agarose beads and washed as described above. Next, the beads were washed with reaction buffer (PBS, 10% glycerol) and resuspended in 500 μL buffer. Five nmol BCN-Cy3 was added to the solution, and the mixture was incubated overnight at 4 °C. After the reaction, excess dye was removed and the bead was washed with wash buffer C (PBS, 0.05% Tween 20) and wash buffer B. The protein was stored at −80 °C after elution and buffer exchange as described above. Labeling of native Lin28 with NHS-Cy3 was performed using the same procedures.

RNA Sequences. RNAs were chemically synthesized by Bioneer. Sequences used for the FRET-based binding assay, high-throughput screening, the electrophoretic mobility shift assay, and the in vitro Dicer processing assay are as follows. PreE-let-7a-1: 5′-UUA GGG UCA CAC CCA CCA CUG GGA GAU AA-3′; PreE-let-7a-1-BHQ-2: 5′-UUA GGG UCA CAC CCA CCA CUG GGA GAU AA-3′-(BHQ-2); Cy5-preE-let-7a-1: (Cy5)-5′-UUA GGG UCA CAC CCA CCA

DOI: 10.1021/jacs.6b06965
J. Am. Chem. Soc. 2016, 138, 13630−13638

CUG GGA GAU AA-3′; Cy5-preE-let-7g: (Cy5)-5′-UGA GGG UCU AUG AUA CCA CCC GGU ACA GGA GAU AA-3′; Biotin-PreE-let-7a-1: (Biotin)-5′-UUA GGG UCA CAC CCA CCA CUG GGA GAU AA-3′. Pre-let-7g: (Phosphate)-5′-UGA GGU AGU AGU UUG UAC AGU UUG AGG GUC UAU GAU ACC ACC CGG UAC AGG AGA UAA CUG UAC AGG CCA CUG CCU UGC-3′.

FRET Assay and High-Throughput Screening. Cy3-Lin28A (25 nM) was mixed with PreE-let-7a-1-BHQ-2 (50 nM) in binding buffer (50 mM Tris·HCl, pH 7.5, 100 mM NaCl, 10 mM β-mercaptoethanol, 1.5% DMSO, 0.01% Tween 20 and 2.6 U recombinant RNase inhibitor [Takara]) in a 50 μL volume. 96-well half area nonbinding black plate with clear bottom [Corning, #3881] was used for the binding reaction and high-throughput screening. The mixture was incubated for 30−60 min at room temperature with mild shaking. Cy3 fluorescence was recorded with a Synergy HT microplate reader [BioTek] with excitation at 530/25 nm and emission at 590/35 nm. High-throughput screening was conducted under the same conditions. Reactions in the presence of 2 μM unlabeled PreE-let-7a-1 or reactions in the absence of any RNA served as positive controls. Reactions with PreE-let-7a-1-BHQ-2 and DMSO served as a negative control. Fluorescent changes induced by compounds were normalized to evaluate the correct inhibitory effects.

Electrophoretic Mobility Shift Assay (EMSA). EMSA was performed to confirm the activities of primary hit compounds and to determine IC_{50} values. Cy5-preE-let-7a-1 and Cy5-preE-let-7g were used as let-7 probes. Ten nM native Lin28A or Lin28B was incubated with 5 nM let-7 probes and compounds at various concentrations in a binding buffer (50 mM Tris·HCl, pH 7.5, 100 mM NaCl, 10 mM β-mercaptoethanol, 2% DMSO, 0.01% Tween 20, 12% glycerol and 5 U recombinant RNase inhibitor [Takara]) in a 50 μL mixture. The mixture was resolved by 4% native acrylamide gel electrophoresis and the Cy5 signal was visualized using Typhoon Trio [GE healthcare].

Quantitative Real-Time PCR of miRNA. Cells were grown in a 12-well plate in the absence and presence of compounds. Total RNA was extracted using TRIzol [Ambion] according to the manufacturer's protocol. Reverse transcription was performed with 35 ng total RNA using TaqMan MicroRNA Reverse Transcription Kit [Applied Biosystems] according to the manufacturer's protocol. Quantitative real-time PCR was performed on a Step One Plus Real-Time PCR System [Applied Biosystems] using a TaqMan Universal Master Mix II [Applied Biosystems] according to the manufacturer's protocol. All the primers and probes for the assay were supplied from Applied Biosystems. The expression levels of mature miRNAs were normalized to that of U6 snRNA.

■ ASSOCIATED CONTENT

Supporting Information

The Supporting Information is available free of charge on the ACS Publications website at DOI: 10.1021/jacs.6b06965.

Additional experimental procedures, primer sequences, supporting figures and tables, synthetic schemes and spectroscopic data (PDF)

■ AUTHOR INFORMATION

Corresponding Author

*sbpark@snu.ac.kr

Notes

The authors declare no competing financial interest.

■ ACKNOWLEDGMENTS

This work was supported by the Creative Research Initiative Grant (2014R1A3A2030423) and the Bio & Medical Technology Development Program (2012M3A9C4048780) through the National Research Foundation of Korea (NRF) funded by the Korean Government (Ministry of Science, ICT & Future Planning). We thank Prof. Se Won Suh and Dr. Kyoung Hoon Kim for providing the genes for Lin28 and technical support. D.L., W.G.B., J.Y.K., and H.P. are grateful for their predoctoral fellowship awarded by the BK21 Plus Program.

■ REFERENCES

(1) Ha, M.; Kim, V. N. *Nat. Rev. Mol. Cell Biol.* **2014**, *15*, 509−524.
(2) Huntzinger, E.; Izaurralde, E. *Nat. Rev. Genet.* **2011**, *12*, 99−110.
(3) van Kouwenhove, M.; Kedde, M.; Agami, R. *Nat. Rev. Cancer* **2011**, *11*, 644−656.
(4) Dong, H. F.; Lei, J. P.; Ding, L.; Wen, Y. Q.; Ju, H. X.; Zhang, X. J. *Chem. Rev.* **2013**, *113*, 6207−6233.
(5) Garzon, R.; Marcucci, G.; Croce, C. M. *Nat. Rev. Drug Discovery* **2010**, *9*, 775−789.
(6) Li, Z. H.; Rana, T. M. *Nat. Rev. Drug Discovery* **2014**, *13*, 622−638.
(7) Li, Q. J.; Chau, J.; Ebert, P. J. R.; Sylvester, G.; Min, H.; Liu, G.; Braich, R.; Manoharan, M.; Soutschek, J.; Skare, P.; Klein, L. O.; Davis, M. M.; Chen, C. Z. *Cell* **2007**, *129*, 147−161.
(8) Thomas, J. R.; Hergenrother, P. J. *Chem. Rev.* **2008**, *108*, 1171−1224.
(9) Heo, I.; Joo, C.; Kim, Y. K.; Ha, M.; Yoon, M. J.; Cho, J.; Yeom, K. H.; Han, J.; Kim, V. N. *Cell* **2009**, *138*, 696−708.
(10) Trang, P.; Medina, P. P.; Wiggins, J. F.; Ruffino, L.; Kelnar, K.; Omotola, M.; Homer, R.; Brown, D.; Bader, A. G.; Weidhaas, J. B.; Slack, F. J. *Oncogene* **2010**, *29*, 1580−1587.
(11) Chen, P. S.; Su, J. L.; Cha, S. T.; Tarn, W. Y.; Wang, M. Y.; Hsu, H. C.; Lin, M. T.; Chu, C. Y.; Hua, K. T.; Chen, C. N.; Kuo, T. C.; Chang, K. J.; Hsiao, M.; Chang, Y. W.; Chen, J. S.; Yang, P. C.; Kuo, M. L. *J. Clin. Invest.* **2011**, *121*, 3442−3455.
(12) Boyerinas, B.; Park, S. M.; Hau, A.; Murmann, A. E.; Peter, M. E. *Endocr.-Relat. Cancer* **2010**, *17*, F19−F36.
(13) Xia, Y.; Zhu, Y.; Zhou, X. Y.; Chen, Y. J. *Tumor Biol.* **2014**, *35*, 5143−5148.
(14) Buechner, J.; Tomte, E.; Haug, B. H.; Henriksen, J. R.; Lokke, C.; Flaegstad, T.; Einvik, C. *Br. J. Cancer* **2011**, *105*, 296−303.
(15) Piskounova, E.; Polytarchou, C.; Thornton, J. E.; LaPierre, R. J.; Pothoulakis, C.; Hagan, J. P.; Iliopoulos, D.; Gregory, R. I. *Cell* **2011**, *147*, 1066−1079.
(16) Viswanathan, S. R.; Daley, G. Q.; Gregory, R. I. *Science* **2008**, *320*, 97−100.
(17) Thornton, J. E.; Gregory, R. I. *Trends Cell Biol.* **2012**, *22*, 474−482.
(18) Chang, H. M.; Triboulet, R.; Thornton, J. E.; Gregory, R. I. *Nature* **2013**, *497*, 244−248.
(19) Ng, S. C.; Daley, G. Q. *Cell Stem Cell* **2013**, *12*, 395−406.
(20) Yu, F.; Yao, H.; Zhu, P.; Zhang, X.; Pan, Q.; Gong, C.; Huang, Y.; Hu, X.; Su, F.; Lieberman, J.; Song, E. *Cell* **2007**, *131*, 1109−1123.
(21) Viswanathan, S. R.; Powers, J. T.; Einhorn, W.; Hoshida, Y.; Ng, T. L.; Toffanin, S.; O'Sullivan, M.; Lu, J.; Phillips, L. A.; Lockhart, V. L.; Shah, S. P.; Tanwar, P. S.; Mermel, C. H.; Beroukhim, R.; Azam, M.; Teixeira, J.; Meyerson, M.; Hughes, T. P.; Llovet, J. M.; Radich, J.; Mullighan, C. G.; Golub, T. R.; Sorensen, P. H.; Daley, G. Q. *Nat. Genet.* **2009**, *41*, 843−848.
(22) Zhang, W. C.; Shyh-Chang, N.; Yang, H.; Rai, A.; Umashankar, S.; Ma, S. M.; Soh, B. S.; Sun, L. L.; Tai, B. C.; Nga, M. E.; Bhakoo, K. K.; Jayapal, S. R.; Nichane, M.; Yu, Q.; Ahmed, D. A.; Tan, C.; Sing, W. P.; Tam, J.; Thirugananam, A.; Noghabi, M. S.; Pang, Y. H.; Ang, H. S.; Mitchell, W.; Robson, P.; Kaldis, P.; Soo, R. A.; Swarup, S.; Hsuen, E.; Lim, B. *Cell* **2012**, *148*, 259−272.
(23) Hayashi, S.; Tanaka, J.; Okada, S.; Isobe, T.; Yamamoto, G.; Yasuhara, R.; Irie, T.; Akiyama, C.; Kohno, Y.; Tachikawa, T.; Mishima, K. *Exp. Cell Res.* **2013**, *319*, 1220−1228.
(24) Zhou, J. B.; Ng, S. B.; Chng, W. J. *Int. J. Biochem. Cell Biol.* **2013**, *45*, 973−978.
(25) Roos, M.; Rebhan, M. A. E.; Lucic, M.; Pavlicek, D.; Pradere, U.; Towbin, H.; Civenni, G.; Catapano, C. V.; Hall, J. *Nucleic Acids Res.* **2015**, *43*, e9.

DOI: 10.1021/jacs.6b06965
J. Am. Chem. Soc. 2016, 138, 13630−13638

(26) Roos, M. Ph.D. Thesis, ETH Zürich, Nr. 22468, Switzerland, 2015.
(27) Roos, M.; Pradère, U.; Ngondo, R. P.; Behera, A.; Allegrini, S.; Civenni, G.; Zagalak, J. A.; Marchand, J.- R.; Menzi, M.; Towbin, H.; Scheuermann, J.; Neri, D.; Caflisch, A.; Catapano, C. V.; Ciaudo, C.; Hall, J. *ACS Chem. Biol.* **2016**, DOI: 10.1021/acschembio.6b00232.
(28) Velagapudi, S. P.; Gallo, S. M.; Disney, M. D. *Nat. Chem. Biol.* **2014**, *10*, 291−297.
(29) Berney, C.; Danuser, G. *Biophys. J.* **2003**, *84*, 3992−4010.
(30) Milroy, L. G.; Grossmann, T. N.; Hennig, S.; Brunsveld, L.; Ottmann, C. *Chem. Rev.* **2014**, *114*, 4695−4748.
(31) Piston, D. W.; Kremers, G. J. *Trends Biochem. Sci.* **2007**, *32*, 407−414.
(32) Sahoo, H. *RSC Adv.* **2012**, *2*, 7017−7029.
(33) Nam, Y.; Chen, C.; Gregory, R. I.; Chou, J. J.; Sliz, P. *Cell* **2011**, *147*, 1080−1091.
(34) Loughlin, F. E.; Gebert, L. F.; Towbin, H.; Brunschweiger, A.; Hall, J.; Allain, F. H. *Nat. Struct. Mol. Biol.* **2012**, *19*, 84−89.
(35) Triboulet, R.; Pirouz, M.; Gregory, R. I. *Cell Rep.* **2015**, *13*, 260−266.
(36) Liu, C. C.; Schultz, P. G. *Annu. Rev. Biochem.* **2010**, *79*, 413−444.
(37) Young, T. S.; Ahmad, I.; Yin, J. A.; Schultz, P. G. *J. Mol. Biol.* **2010**, *395*, 361−374.
(38) Johnson, D. B. F.; Xu, J. F.; Shen, Z. X.; Takimoto, J. K.; Schultz, M. D.; Schmitz, R. J.; Xiang, Z.; Ecker, J. R.; Briggs, S. P.; Wang, L. *Nat. Chem. Biol.* **2011**, *7*, 779−786.
(39) O'Donoghue, P.; Ling, J.; Wang, Y. S.; Soll, D. *Nat. Chem. Biol.* **2013**, *9*, 594−598.
(40) Cridge, A. G.; Major, L. L.; Mahagaonkar, A. A.; Poole, E. S.; Isaksson, L. A.; Tate, W. P. *Nucleic Acids Res.* **2006**, *34*, 1959−1973.
(41) Dommerholt, J.; Schmidt, S.; Temming, R.; Hendriks, L. J. A.; Rutjes, F. P. J. T.; van Hest, J. C. M.; Lefeber, D. J.; Friedl, P.; van Delft, F. L. *Angew. Chem., Int. Ed.* **2010**, *49*, 9422−9425.
(42) Zhang, J. H.; Chung, T. D. Y.; Oldenburg, K. R. *J. Biomol. Screening* **1999**, *4*, 67−73.
(43) Kim, J.; Kim, H.; Park, S. B. *J. Am. Chem. Soc.* **2014**, *136*, 14629−14638.
(44) Pagano, J. M.; Clingman, C. C.; Ryder, S. P. *RNA* **2011**, *17*, 14−20.
(45) Park, S. O.; Kim, J.; Koh, M.; Park, S. B. *J. Comb. Chem.* **2009**, *11*, 315−326.
(46) Nowak, J. S.; Choudhury, N. R.; Alves, F. D.; Rappsilber, J.; Michlewski, G. *Nat. Commun.* **2014**, *5*, 3687.
(47) Warrander, F.; Faas, L.; Kovalevskiy, O.; Peters, D.; Coles, M.; Antson, A. A.; Genever, P.; Isaacs, H. V. *Dev. Dyn.* **2016**, *245*, 34−46.
(48) Melton, C.; Judson, R. L.; Blelloch, R. *Nature* **2010**, *463*, 621−626.
(49) Guan, L. R.; Disney, M. D. *ACS Chem. Biol.* **2012**, *7*, 73−86.
(50) Clingman, C. C.; Deveau, L. M.; Hay, S. A.; Genga, R. M.; Shandilya, S. M. D.; Massi, F.; Ryder, S. P. *eLife* **2014**, *3*, e02848.

DOI: 10.1021/jacs.6b06965
J. Am. Chem. Soc. 2016, 138, 13630−13638